1D chains and an open 3D network from poly(diethylamidinium) cations and polycarboxylate anions

Meabh K. S. Perry-Britton, Jessica J. Du and Nicholas G. White*

New monotopic, ditopic, and tetratopic diethylamidinium building blocks were prepared and their interactions with (poly)carboxylates studied in solution and by crystallisation to give hydrogen-bonded networks. Crystallisation of the bis(diethylamidinium) tecton with terephthalate or biphenyldicarboxylate gave 1D hydrogen-bonded chains where the diethylamidinium groups adopted *E/E* conformations allowing for $R_2^2(8)$ hydrogen bonding with the anion. In contrast, 3D networks had *E/Z* diethylamidinium conformations, limiting hydrogen bonding to single-point interactions. Despite this, an open network structure was formed where approximately half of the unit cell volume was occupied by disordered solvent molecules. A survey of the Cambridge Structural Database revealed that both *E/E* and *E/Z* arrangements are common, while DFT calculations suggest that the *E/E* conformation is ~ 13 kJ mol^{-1} higher in energy than the *E/Z* conformation for both dimethylamidiniums and diethylamidiniums in the gas phase. Factors that contribute to the favourability of *E/E* and *E/Z* arrangements in the solid state are discussed, specifically with reference to the design of open networks.

Introduction

Despite decades of interest in hydrogen-bonded frameworks (HOFs),[1–4] there are relatively few pairs of charged functional groups that have been shown to reliably give frameworks assembled through charge-assisted hydrogen bonding.[5] Examples of pairs of ions that have proven useful include guanidinium/sulfonate,[6,7] ammonium/halide,[8,9] pyridinium/carboxylate,[10,11] ammonium/carboxylate,[12,13] and ammonium/sulfonate.[14–16] However, with the notable exception of Ward's guanidinium/sulfonate systems,[6,7] there are still relatively few examples reported for each of these groups.

Building on prior work that investigated the use of cyclic amidiniums and used them to prepare 1D and 2D hydrogen-bonded nets,[17–19] in 2017 we reported 3D frameworks assembled using amidinium···carboxylate hydrogen bonds.[20] Subsequent work by a range of groups has revealed that frameworks can be prepared from amidinium cations and (hydrogen)carbonate,[21,22] carboxylate,[23–25] phosphonate[26–29] and sulfonate[26,30,31] anions in a predictable manner. In particular, a wide range of amidinium/carboxylate materials have been reported. These amidinium-based frameworks have found applications in a range of fields including atmospheric water harvesting,[30] removal of toxins from water[32,33] and enzyme encapsulation.[25,34,35]

In all cases, these frameworks have been prepared from "unsubstituted" amidinium groups where there are no substituents on the amidinium nitrogen atoms, *i.e.* H_2N^+=C(R)–NH_2. It is relatively simple to prepare substituted amidinium derivatives, *i.e.* R–HN^+=C(R)–NH–R, and Yashima has used these to prepare a range of self–assembled supramolecular structures.[36,37] These R substituents can adopt several conformations, specifically *E/E*, *E/Z* or *Z/Z* (Figure 1), and a survey of the CSD indicates that both *E/E* and *E/Z* arrangements are common (see later). Solution studies in aprotic solvents show that substituted amidinium groups typically have an *E/Z* conformation in the absence of a hydrogen bonding guest, but that addition of a good hydrogen bond acceptor such as a carboxylate results in a switch to the *E/E* conformation.[36–40]

We recently studied the assembly of poly(dimethylamidinium) cations with polycarboxylate anions:[41] we found that in CD_3CN or d_6-DMSO, addition of benzoate to a simple dimethylamidinium compound caused the expected *E/Z* to *E/E* switch. However, when we crystallised the poly(dimethylamidinium) compounds with polycarboxylates from ethanol, water or ethanol/water mixtures, all structures had the *E/Z* geometry (we were unable to obtain crystals from aprotic solvents). Previously, Grosu and Legrand showed that bis(diisopropyl)amidinium compounds remained in the *E/Z* geometry in the presence of dicarboxylates in CD_3OD solution, and in the crystalline state.[42]

In this work, we expand our study to diethylamidinium derivatives and show that in some cases it is possible to obtain *E/E* geometries when crystallising from polar protic solvents. DFT studies indicate that this is not due to a significantly different energy barrier between conformations for methyl vs. ethyl derivatives, but rather appears to be due to crystal packing effects. We also show that *E/Z* geometries do not preclude the formation of open structures, obtaining a 3D diamondoid network where 48% of the unit cell volume is occupied by disordered solvent molecules.

Research School of Chemistry, Australian National University, Canberra, ACT, 2601, Australia. Email: nicholas.white@anu.edu.au; URL: www.nwhitegroup.com.

† Supplementary Information available: [characterisation data, successful and unsuccessful crystallisation conditions, details of solution NMR studies, SCXRD studies, CSD searches, DFT calculations].

Results and Discussion

Synthesis of building blocks

The amidinium building blocks were synthesised from the corresponding *N*-ethyl amides, which were themselves synthesised from the corresponding commercially-available carboxylic acids (Scheme 1). Briefly, the carboxylic acids were converted to the corresponding acid chlorides by heating in thionyl chloride and these were then immediately reacted with commercially-available aqueous ethyl amine solution to give the amides in good yields (72 – 97%). These amides were then converted to the imidoyl chloride by heating in thionyl chloride and again immediately reacted with aqueous ethyl amine to give the diethylamidines, which were protonated to give diethylamidiniums in moderate to good overall yields (58 – 78%). In the case of **^{Et}biphen·Cl$_2$**, we were able to obtain single crystals, which revealed that the diethylamidinium groups have the *E/Z* conformation in the solid state (Figure S32).

Solution NMR studies

^{1}H and ^{13}C NMR spectra show that **^{Et}model·BPh$_4$**, **^{Et}biphen·Cl$_2$** and **^{Et}tetra·Cl$_4$** all adopt the *E/Z* conformation in solution, as evidenced by the presence of two sets of signals for the ethyl groups. Heating **^{Et}biphen·Cl$_2$** to 80 °C in D_2O did not result in these peaks becoming equivalent (Figure S25), and adding a large excess (up to 100 equivalents) of sodium benzoate in this solvent did not result in a switch from the *E/Z* to *E/E* conformation (Figure S26, similar results were previously observed with the methyl-substituted analogues[41]). In contrast, adding benzoate to **^{Et}model·BPh$_4$** in CD_3CN or d_6-DMSO results in the ethyl peaks becoming equivalent and small shifts in the aryl C–H resonances (Figures S27 – S30). These changes are consistent with an interaction with between **^{Et}model$^+$** and **BzO$^-$** in these aprotic solvents resulting in a switch from the *E/Z* to *E/E* conformation. Conducting quantitative ^{1}H NMR binding experiments in CD_3CN indicated binding was too strong to quantify using NMR titrations ($K_a > 10^4$ M^{-1}), while fitting the peak movements observed in d_6-DMSO to a 1:1 isotherm using *Bindfit*[43] indicated binding was moderately strong ($K_a = 739 \pm 77$ M^{-1}, Figure S29).

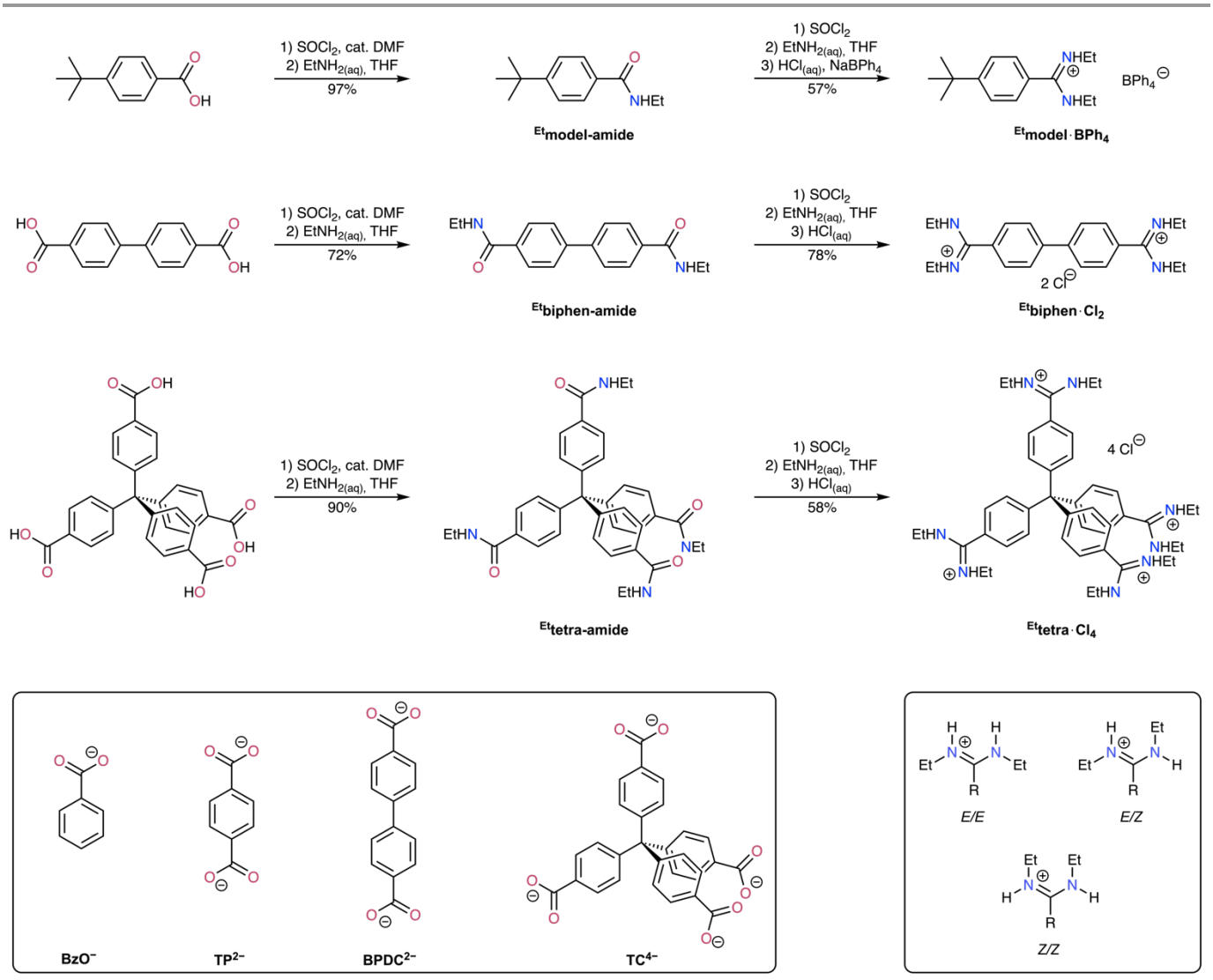

Scheme 1. Synthesis of new amidinium building blocks; insets: structure of anions used and possible geometries of diethylamidinium groups.

These values are consistent with those previously observed for **^{Me}model^{+}** (K_a = 869 ± 66 M^{-1}).[41] Cooling a 1:1 mixture of **^{Et}model·BPh$_4$** and **TBA·BzO** in CD_3CN to −20 or − 40 °C resulted in distinct sets of peaks being visible for bound and free **^{Et}model^{+}** (Figure S31); by integrating these peaks we were able to estimate an association constant of approximately 30,000 M^{-1} at these temperatures (ESI Section 2.4.2). Again, this behaviour and these values are very similar to what was observed in analogous experiments with **^{Me}model^{+}**.[41]

Crystallisation of 1D H-bonded chains

We initially studied the crystallisation of diamidinium compound **^{Et}biphen^{2+}** with the linear dicarboxylates terephthalate^{2-} (**TP^{2-}**) and biphenyldicarboxylate^{2-} (**BPDC^{2-}**) in ethanol and water, as these conditions had proven successful for the analogous dimethylamidinium-containing systems.[41] Tables S1 – S6 detailing all attempted crystallisation conditions are provided in Section 1.4 of the ESI, but briefly, we only ever observed crystals in ethanol at quite high concentrations (10 or 20 mM), and crystals took several weeks to form. Using these conditions, we obtained crystals of both **^{Et}biphen·TP** and **^{Et}biphen·BPDC**. Interestingly, in both cases, the diethylamidinium groups of **^{Et}biphen^{2+}** adopt the *E/E* conformation, allowing "paired" $\boldsymbol{R_2^2(8)}$ hydrogen bonding interactions, which assemble the structures into 1D hydrogen-bonded chains (Figure 1). Hydrogen bonds are similar in length to those observed in crystal structures of unsubstituted amidinium groups interacting with carboxylate anions (H···O distances 1.78 – 1.95 Å, 66 – 72% of the sum of the vdW radii[44] of H and O). The structure of **^{Et}biphen·BPDC** is close-packed, while the structure of **^{Et}biphen·TP** contains 1D channels that are filled with ill-defined electron density. PLATON-SQUEEZE was used to include this electron density,[45] which comprises ~ 30% of the unit cell volume in the refinement.

We were able to scale up the crystallisation of **^{Et}biphen·TP** at 20 mM and isolate this in modest yield (36%). PXRD experiments indicate that the network re-arranges to an unidentified crystalline phase upon removal of the solvent from the channels by drying (Figure S20). In the case of **^{Et}biphen·BPDC**, numerous crystallisations (Table S2) reproducibly gave only a small number of small crystals even at concentrations as high as 20 mM, and so we were never able to isolate a bulk sample.

Crystallisation of 3D networks

Encouraged by the *E/E* conformations and $\boldsymbol{R_2^2(8)}$ hydrogen bonding interactions of the diethylamidinium groups in **^{Et}biphen·TP** and **^{Et}biphen·BPDC**, we next attempted to crystallise networks/frameworks with hydrogen bonding in three dimensions. Attempts to crystallise **^{Et}biphen^{2+}** with the tetrahedral tetracarboxylate **TC^{4-}** (structure shown in Scheme 1) in ethanol or water did not give precipitates (Table S3); crystallisation of **^{Et}tetra^{4+}** with **TP^{2-}** also did not give precipitates in ethanol or water (Table S4). However, when we crystallised the tetrahedral tetra-amidinium **^{Et}tetra^{4+}** with **BPDC^{2-}** or **TC^{4-}** in ethanol, we obtained single crystals (Tables S5 and S6).

Crystal structure of ^{Et}tetra·(^{H}BPDC)$_4$: Disappointingly, in the crystal structure of **^{Et}tetra·(^{H}BPDC)$_4$**, all diethylamidinium groups adopt an *E/Z* conformation. Spontaneous mono-protonation of the dicarboxylate has occurred, resulting in a 4:1 stoichiometry between the **^{H}BPDC^{-}** anion and the tetra-cation (Figure 2) with one **^{H}BPDC^{-}** anion and one quarter of a **^{Et}tetra^{4+}** cation in the asymmetric unit. Both crystallographically-independent amidinium N–H hydrogen atoms hydrogen bond to oxygen atoms with the "forwards-facing" N–H hydrogen bonding to a carboxylic acid group (H···O = 1.97 Å, 73% of the sum of the vdW radii[44] of H and O) and the "sideways-facing" N–H hydrogen bonding to a carboxylate group (H···O = 1.88 Å, 70% of the sum of the vdW radii[44] of H and O). The **^{H}BPDC^{-}** anions form 1D chains linked by anti-electrostatic[46] O–H···O^{-} hydrogen bonds between carboxylic acid and carboxylate groups; these distances are typical for these kind of O–H···O^{-} hydrogen bonds[47] (H···O = 1.52 Å, 56% of the sum of the vdW radii[44] of H and O, O···O^{-} = 2.447(1) Å). The overall structure packs relatively densely, with no solvent included in the structure. Generally the structure is quite similar to that formed from the analogous tetrakis(dimethylamidinium) cation and biphenyldicarboxylate, *i.e.* **^{Me}tetra·(^{H}BPDC)$_4$**, which features similar spontaneous protonation of the anion and a similar hydrogen bonding arrangement.[41]

We conducted numerous crystallisations to try and obtain a bulk sample of **^{Et}tetra·(^{H}BPDC)$_4$** (Table S5), but were unsuccessful. We tried both the 1:2 ratio of **^{Et}tetra^{4+}** and **BPDC^{2-}** used in our initial crystallisation and the 1:4 ratio found in the crystal structure. We also tried adding acetic acid as a proton source to facilitate formation of the **^{H}BPDC^{-}** anion found in the crystal structure. At sub-stoichiometric amounts of acetic acid, we obtained only amorphous material, while when we used one equivalent of acid per **BPDC^{2-}** anion we obtained only the carboxylic acid **^{H2}BPDC** (as determined by ^{1}H NMR spectroscopy and PXRD studies).

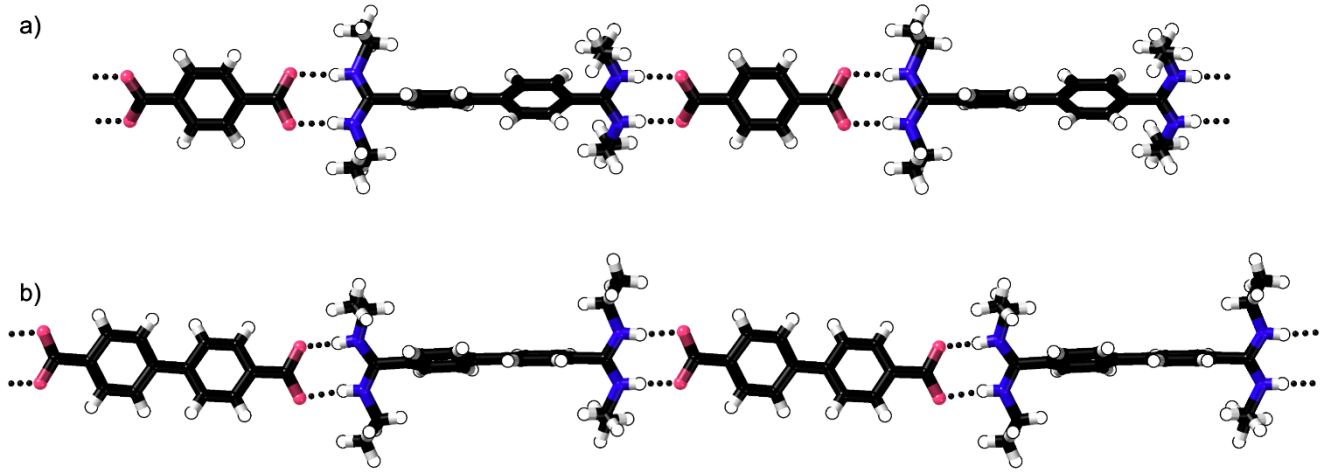

Figure 1. X-ray crystal structures of ^{Et}**biphen·TP** and ^{Et}**biphen·BPDC.** Disorder in the ethyl groups of ^{Et}**biphen**$^{2+}$ in ^{Et}**biphen·TP** is omitted for clarity, PLATON-SQUEEZE[45] was used in the refinement of ^{Et}**biphen·TP**.

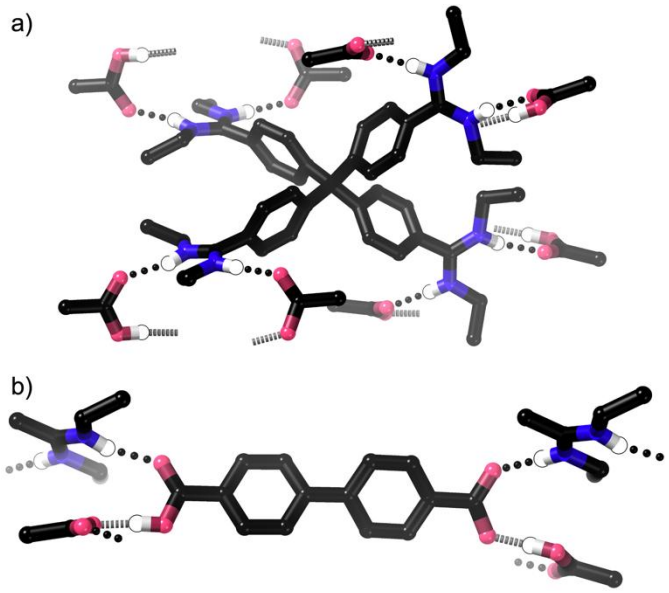

Figure 2. Two views of the X-ray crystal structure of ^{Et}**tetra·(**^{H}**BPDC)$_4$**: a) view showing the arrangement of carboxylate/carboxylic acid groups around the central tetra-amidinium cation; b) view showing the arrangement around a single ^{H}**BPDC**$^{-}$ anion (N–H···O hydrogen bonds are shown as black dotted lines, O–H···O^{-} hydrogen bonds are shown as dashed grey lines, disorder of one of the ethyl groups of ^{Et}**tetra**$^{4+}$ is omitted for clarity).

Crystal structure of ^{Et}tetra·TC: We were able to obtain relatively large single crystals of ^{Et}**tetra·TC**, however these appeared to lose solvent rapidly and diffraction intensity dropped off dramatically at high angle. We collected several X-ray diffraction datasets under various conditions including cold-mounting crystals and using synchrotron radiation, but were never able to obtain diffraction data beyond 0.95 Å resolution. The low diffraction resolution and the presence of relatively large voids filled with diffuse electron density (which we attribute to disordered solvent molecules, and which was included in the model using PLATON-SQUEEZE[45]) mean that the structure is of relatively low quality, however the molecular structure and packing can be determined unambiguously.

All diethylamidinium groups have the *E/Z* conformation. The structure has the form of a diamondoid net assembled by hydrogen bonding between the "forwards-facing" hydrogen atoms of ^{Et}**tetra**$^{4+}$ and carboxylate oxygen atoms of **TC**$^{4-}$ (Figure 3)**.** Hydrogen bond lengths are similar to those for other amidinium···carboxylate interactions,[23,41] noting that the data are of relatively low quality so these values are likely inexact (H···O = 1.77 – 1.93 Å, 66 – 72% of the sum of the vdW radii[44]). Four of these diamondoid networks interpenetrate, which is a lower degree of interpenetration than the analogous framework prepared from the unsubstituted tetra-amidinium building block (without ethyl groups), *i.e.* **tetra·TC**, which is six-fold interpenetrated.[23] As a result, large channels are present, with these voids comprising 48% of the unit cell volume, according to PLATON-SQUEEZE[45] analysis (this compares with 29% in **tetra·TC**[23]). This value is quite high, particularly given the multiple competing hydrogen bonding arrangements that could potentially form. We were able to isolate a "bulk" sample of ^{Et}**tetra·TC** in high yield (92%), but unfortunately the material lost all crystallinity upon drying. Presumably the single-point hydrogen bonding interactions are not sufficiently strong to support the low density network when solvent is removed.

Given that solution studies showed that diethylamidiniums switch from *E/Z* to *E/E* geometries in the presence of carboxylate anions in polar aprotic solvents (acetonitrile and DMSO), we attempted crystallisations using ^{Et}**tetra·Cl$_4$** and **TP**$^{2-}$, **BPDC**$^{2-}$ and **TC**$^{4-}$ in aprotic solvents. Unfortunately, ^{Et}**tetra·Cl$_4$** is not appreciably soluble in acetonitrile or DMF and attempted crystallisations in DMSO rapidly formed amorphous precipitates even at low concentrations (sub-mM, Tables S4 – S6).

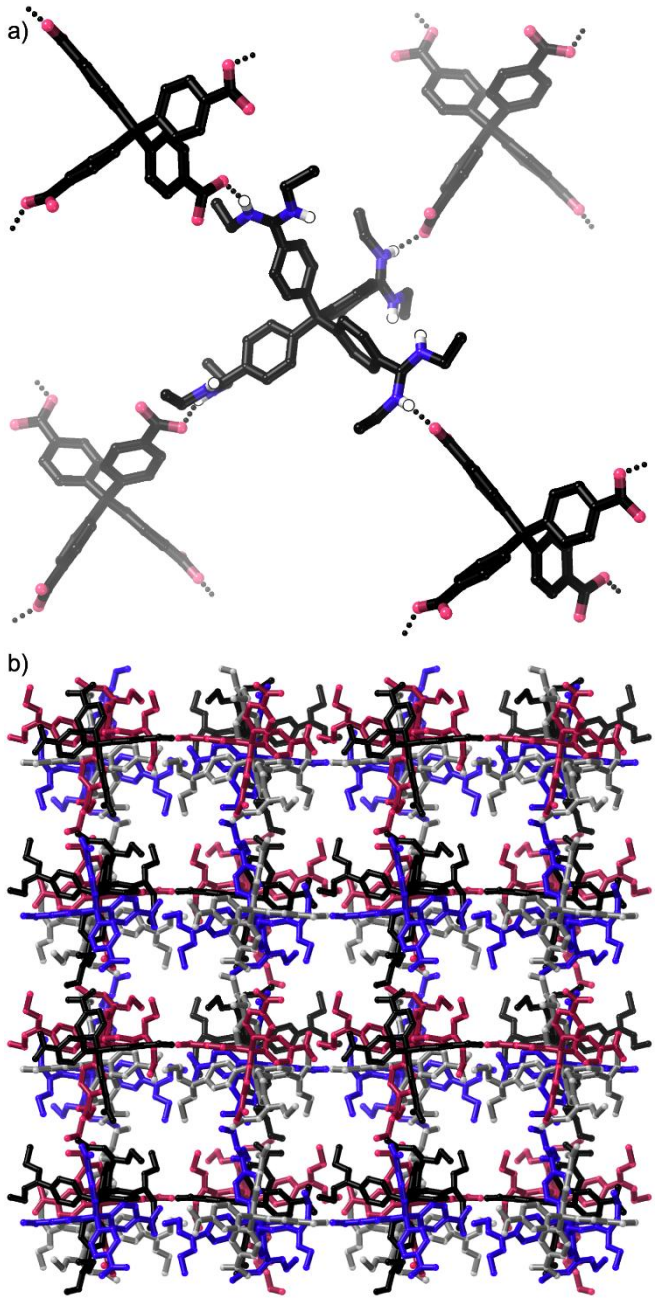

Figure 3. Views of the X-ray crystal structure of ^{Et}**tetra·TC**: a) view showing the hydrogen bonding interactions that assemble the diamondoid network; b) view showing the packing and the four interpenetrated diamondoid nets, with each net shown in a different [most hydrogen atoms in a) and all hydrogen atoms in b) are omitted for clarity, PLATON-SQUEEZE[45] was used].

Cambridge Structural Database survey

We conducted a survey of the Cambridge Structural Database[48] (CSD, Version 6.00, April 2025) to look at disubstituted amidiniums and their conformations (see ESI Section 4 for search fragments and full details). Briefly, these reveal that 17/31 dialkylamidinium structures adopt an *E/Z* conformation while 14/31 have the *E/E* conformation and none have the *Z/Z* conformation. There are five diarylamidinium structures in the CSD, two have the *E/E* conformation and three have the *Z/Z* conformation. In addition, we recently published 15 structures of dimethylamidinium compounds (too recent to be picked up in this CSD search), and all of these have the *E/Z* conformation. While there are only a small number of datapoints available, it does seem that in general coordinating anions, and in particular carboxylates, favour the *E/E* conformation (Table S8), as would be expected. However, this is clearly affected by factors such as protic solvents that can compete with the coordinating anion, and there are several carboxylate-containing structures that have an *E/Z* arrangement.

Separately, we investigated the effect of methyl and ethyl substituents on the angles between the amidinium group and phenyl ring to which it is attached in benzamidinium derivatives (both in the CSD and in our data, see ESI Section 4 for full details). While a wide range of values are observed, on average the mean plane angle between diethylamidinium groups and their attached phenyl substituent is slightly larger (68(3)°) than between dimethylamidinium groups and phenyl substituents (59(2)°). The angle between unsubstituted amidinium groups and phenyl substituents is much lower (33(1)°).

DFT calculations

We observed the *E/E* conformation of diethylamidinium groups in ^{Et}**biphen·TP** and ^{Et}**biphen·BPDC**, but never observed this conformation in 15 X-ray crystal structures of dimethylamidinium compounds (11 of these are crystal structures of carboxylate salts). We therefore wondered whether there was a lower energy difference between the *E/Z* and *E/E* conformations for diethylamidinium groups than dimethylamidiniums. To probe this, we ran DFT calculations on the simplified model cations ^{Me}**calc**$^{+}$ and ^{Et}**calc**$^{+}$ (Figure 4) as well as isopropyl- and phenyl-substituted analogues (ESI Section 5) using either the M06-2X[49] or ωB97X-D[50] density functionals and the 6-311+G** basis set. Full details are provided in the ESI, but briefly the difference in energy between the *E/Z* and *E/E* conformation appears to be very similar for both dimethyl amidinium and diethylamidinium cations with the *E/Z* conformation calculated to be ~ 13 kJ mol^{-1} more favourable in the gas phase and ~ 9 kJ mol^{-1} more favourable in implicit water (C-PCM model) for both ^{Me}**calc**$^{+}$ and ^{Et}**calc**$^{+}$. It therefore appears that the observed *E/Z* conformation in the crystal structures of ^{Et}**biphen·TP** and ^{Et}**biphen·BPDC** occurs due to some other aspect of the crystal packing rather than a reduced unfavourability of the *E/Z* conformation. This is consistent with our solution NMR studies which showed very similar behaviour for ^{Et}**model**$^{+}$ and ^{Et}**biphen**$^{2+}$ to that previously observed for ^{Me}**model**$^{+}$ and ^{Me}**biphen**$^{2+}$.[41]

More generally, these values of ~ 13 kJ mol^{-1} in the gas phase and ~ 9 kJ mol^{-1} are broadly similar to the interaction energies for weak host–guest binding (9 and 13 kJ mol^{-1} correspond to K_a values of 40 and 200 M^{-1}, respectively at 298 K). While the difference in energy between the conformers will vary a little with solvent, it is unsurprising that carboxylate binding in an aprotic solvent is strong enough to overcome this value, while the essentially negligible binding in water/alcohols is not enough to switch conformation in solution.

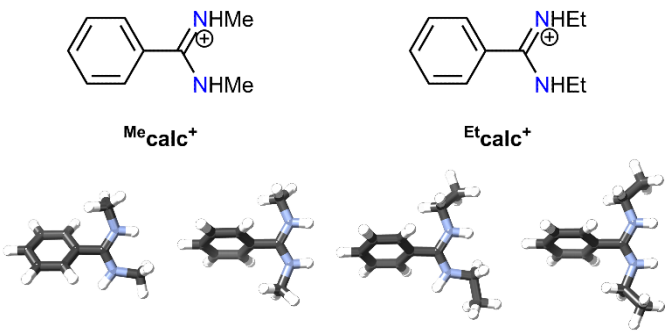

^{Me}**calc**$^{+}$ ^{Et}**calc**$^{+}$

Compound	Functional	Energy difference (kJ mol^{-1})
^{Me}**calc**$^{+}$	ωB97X-D	12.3
^{Me}**calc**$^{+}$	M06-2X	13.0
^{Et}**calc**$^{+}$	ωB97X-D	12.5
^{Et}**calc**$^{+}$	M06-2X	13.2

Figure 4. Structures of *E/Z* and *E/E* conformers of ^{Me}**calc**$^{+}$ and ^{Et}**calc**$^{+}$ calculated in the gas phase (M06-2X/6-311G+**) and calculated energy differences between the *E/Z* and *E/E* conformers. In all cases, the *E/Z* conformer is lower in energy. Further details and information, including calculations in implicit water, are provided in the ESI.

Discussion

DFT calculations suggest that the difference in energy between the *E/E* and *E/Z* conformations is essentially the same for the methyl- and ethyl-functionalised amidiniums (~ 13 kJ mol^{-1}). In solution in aprotic solvents, interaction with carboxylates is favourable enough to overcome this modest energy barrier causing a change from the *E/Z* to *E/E* conformation, presumably to allow $R_2^2(8)$ hydrogen bonding with the anion. In this work, we have observed both *E/Z* and *E/E* conformations of diethylamidinium groups in the solid state, where similar studies with related dimethylamidinium groups gave only the *E/Z* conformation.[41] We suggest that the most likely cause for formation of the otherwise-unfavoured *E/E* conformation in the 1D H-bonded chains ^{Et}**biphen·TP** and ^{Et}**biphen·BPDC** are oft-invoked "crystal packing effects." That is, favourable interactions in other parts of the structure can compensate for the less-favoured *E/E* conformation. We note that there are several other factors that may also have an effect, including the different solubility of the diethylamidinium-containing molecules: it is notable that quite high concentrations were needed to obtain crystals in this work, significantly higher than for dimethylamidinium-containing components,[41] which are themselves much higher than for the parent unsubstituted amidinium components.[23,33]

Based on DFT studies and CSD searches, it appears that the barrier for *E/Z* to *E/E* switching is relatively small, and can be overcome by the presence of a good hydrogen bond acceptor that favours an *E/E* arrangement. What makes a good hydrogen bond acceptor is dependent on the solvent, so when crystallising from alcohols or water, even a carboxylate anion is not enough in most cases, presumably due to competition from the hydrogen bonding solvent. When attempting to form networks, there is a difficulty as a competitive solvent is needed both to dissolve the highly-charged tectons and to prevent rapid precipitation of amorphous materials, but this then minimise interactions with the anion and so often results in the *E/Z* conformation. In the current work, even using DMSO, amorphous precipitates formed rapidly. For discrete systems rather than frameworks, this is not an issue, and so use of an aprotic solvent and hydrogen bonding guest will generally favour the *E/E* conformation.[36,37,40]

A final point of note is that networks formed from unsubstituted amidinium and dimethylamidinium components show a tendency towards solvatomorphism where multiple crystal phases form in the same or very similar crystallisation conditions. While we have a reasonably small number of datapoints in the current study (four networks from 78 sets of attempted crystallisation conditions), we only observed one crystal phase of each network. Possibly the bulkier ethyl groups act to reduce the number of possible crystal structures that can form, or perhaps the reduced number of conditions that lead to crystals mean we simply have not found these alternative solvatomorphs yet.

Conclusions

This study provides insight into the conformational preferences of disubstituted amidinium derivatives. CSD searches reveal that both *E/Z* and *E/E* conformations are relatively common in the solid state, while the *Z/Z* conformation has not been observed for dialkylamidiniums but has been observed for diarylamidiniums. DFT calculations indicate that there is a modest barrier to reach the *E/E* conformation for methyl or ethyl-substituted amidiniums. Solution studies show that in polar aprotic solvents (acetonitrile, dimethylsulfoxide), interaction with carboxylate anions is favourable enough to drive an *E/Z* to *E/E* transformation, but in water this does not occur even in the presence of a large excess of carboxylate. For the structures in the CSD it appears that the amidinium conformation depends on a variety of factors including the nature of the substituent, the solvent used, and the presence or absence of anions that can hydrogen bond favourably to the *E/E* conformer.

In the solid state, we observed both *E/Z* and *E/E* conformations of diethylamidinium groups in crystals with carboxylate anions grown from ethanol. This resulted in the formation of 1D H-bonded chains containing *E/E* amidinium groups and two different 3D networks with *E/Z* amidiniums. The structure of ^{Et}**tetra·(**^{H}**BPDC)$_4$** is densely-packed and assembled through amidinium···carboxylate hydrogen bonding and short hydrogen bonds between carboxylic acid and carboxylate groups on mono-protonated ^{H}**BPDC**$^{-}$ anions. In contrast, the structure of ^{Et}**tetra·TC** is an open 3D network assembled through single-point amidinium···carboxylate hydrogen bonds where approximately half of the structure is made up of disordered solvent.

While in this case ^{Et}**tetra·TC** has poor stability and loses crystallinity upon drying, it demonstrates that open network structures can be assembled using these single-point hydrogen bonds. More stable materials may be attainable using different amidinium substituents that can act to stabilise a resulting framework.

Experimental

General remarks

The TBA^+ salts of the polycarboxylate anions **TBA_2·TP**,[51] **TBA_2·BPDC**[23] and **TBA_4·TC**[52] were prepared as described previously. **Na·BzO** and **TBA·BzO** used in solution binding studies (Section 2) were purchased commercially and used as received. Details of instrumentation and characterisation data/spectra are provided in the ESI.

Synthesis of ^{Et}model-amide: *This compound has been reported previously but was prepared by a different method.* Thionyl chloride (8 mL) was added to 4-*tert*-butylbenzoic acid (0.535 g, 3.00 mmol), followed by DMF (7 drops). The resulting solution was heated to reflux for 3 hours and then the solution cooled to room temperature thionyl chloride was removed by vacuum distillation. The resulting white solid was dissolved in THF (40 mL) and added to ethyl amine (2 mL, 68 – 72% in water). After 15 minutes, the mixture was diluted with water (14 mL) and $HCl_{(aq)}$ (36%, 1.9 mL). The THF was removed on a rotary evaporator to give a brown oil suspended in the aqueous phase. This was extracted with EtOAc (3 × 15 mL) and the combined organic phases washed with brine (15 mL), dried ($MgSO_4$) and then taken to dryness under reduced pressure to give **^{Et}model-amide** as a pale brown oil that crystallised on standing. Yield: 0.598 g (2.91 mmol, 97%).

^{1}H NMR (d_6-DMSO): 8.36 (t, *J* = 5.6 Hz, 1H), 7.76 (d, *J* = 8.5 Hz, 2H), 7.45 (d, *J* = 8.5 Hz, 2H), 3.27 (dq, *J* = 7.2, 5.6 Hz, 2H), 1.29 (s, 9H), 1.11 (t, *J* = 7.2 Hz, 3H) ppm. ^{13}C{^{1}H} NMR (d_6-DMSO): 165.9 , 153.8, 132.1, 127.0, 125.0, 34.7, 34.0, 31.1, 15.0 ppm. HRESI-MS (pos.): *m*/z = 206.1538, calc. for $[C_{13}H_{18}NO{\cdot}H]^+$ = 206.1540. ATR-IR (*inter alia*): 1634 (strong), 1543 (strong) cm^{-1}.

Synthesis of ^{Et}model·BPh_4: Thionyl chloride (5 mL) was added to **^{Et}model-amide** (0.596 g, 2.90 mmol) and the solution heated to reflux for 3 hours during which time an orange solution formed. The solution was then cooled to room temperature and the thionyl chloride removed by vacuum distillation to give a red oil. This was dissolved in THF (10 mL) and added dropwise to a solution of ethylamine (3 mL, 68 – 72% in water) at −10 °C. After stirring at this temperature for 1 hour, the solution was allowed to warm to room temperature overnight to give a pale brown solution containing a brown oil. This was taken to dryness under reduced pressure to give a yellow powder. $NaOH_{(aq)}$ (1 M, 20 mL) was added and the mixture extracted with EtOAc (3 × 10 mL). The combined organic phases were washed with brine (15 mL), dried ($MgSO_4$) and taken to dryness under reduced pressure. The resulting brown oil was dissolved in $HCl_{(aq)}$ (1 M, 3 mL) and water (20 mL) and a solution of $NaBPh_4$ (1.0 g, 3.0 mmol) in water (20 mL) was added resulting in the formation of a brown solid. This was dissolved in acetone (25 mL), and added to water (50 mL) to precipitate an off-white powder, which was isolated by filtration, washed with water (3 × 10 mL) and dried *in vacuo* to give **^{Et}model·BPh_4**. Yield: 0.910 g (1.65 mmol, 57%).

^{1}H NMR (d_6-DMSO): 9.54 (br. s, 1H), 9.05 (br. s, 1H), 7.64 (d, *J* = 8.5 Hz, 2H), 7.50 (d, *J* = 8.5 Hz, 2H), 7.21 (br. s, 8H), 6.95 (dd, *J* = 7.4, 7.2 Hz, 8H), 6.81 (t, *J* = 7.2 Hz, 4H), 3.39 (obscured by water signal), 3.15 (dq, *J* = 7.1, 5.5 Hz, 2H), 1.33 (s, 9H), 1.24 (t, *J* = 7.1 Hz, 3H), 1.09 (t, *J* = 7.1 Hz, 3H) ppm. ^{13}C{^{1}H} NMR (d_6-DMSO): 162.6 – 164.1 (m), 154.9, 135.6, 127.9, 125.9, 125.6, 125.2 – 125.4 (m), 121.5, 37.5, 34.8, 30.8, 15.1, 12.8 ppm. HRESI-MS (pos.): *m*/z = 223.2008, calc. for $[C_{13}H_{21}N_2]^+$ = 233.2013. HRESI-MS (neg.): *m/z* = 319.1663, calc. for $[C_{24}H_{20}B]^-$ = 319.1663. ATR-IR (*inter alia*): 1629 (strong) cm^{-1}.

Synthesis of ^{Et}biphen-amide: Thionyl chloride (10 mL) was added to biphenyl dicarboxylic acid (1.12 g, 5.00 mmol) followed by DMF (5 drops). The mixture was heated to reflux for 3 hours during which time a pale yellow suspension formed. The reaction was cooled to room temperature and the thionyl chloride was removed by vacuum distillation to give a yellow solid. This was dissolved in THF (30 mL) and added to ethylamine solution (6 mL, 68 – 72% in water) in an ice-bath. After stirring in the ice-bath for 15 minutes, the mixture was diluted with water (24 mL) and then $HCl_{(aq)}$ (36%, 3.2 mL) resulting in the formation of a fluffy white powder. This was isolated by filtration, washed with water (2 × 15 mL) and then methanol (2 × 15 mL) and then air-dried to give **^{Et}biphen-amide**. Yield: 1.06 g (3.58 mmol, 72%).

^{1}H NMR (d_6-DMSO): 8.54 (t, *J* = 5.6 Hz, 2H), 7.95 (d, *J* = 8.4 Hz, 4H), 7.83 (d, *J* = 8.4 Hz, 4H), 3.31 (obscured by water peak), 1.14 (t, *J* = 7.2 Hz, 6H) ppm. ^{13}C{^{1}H} NMR (d_6-DMSO): 165.4, 141.5, 133.9, 127.8, 126.6, 34.1, 14.8 ppm. HRESI-MS (pos.): *m/z* = 297.1612, calc. for $[C_{18}H_{20}N_2O_2{\cdot}H]^+$ = 297.1598. ATR-IR (*inter alia*): 1631 (strong), 1537 (strong) cm^{-1}.

Synthesis of ^{Et}biphen·Cl_2: Thionyl chloride (4 mL) was added to **^{Et}biphen-amide** (0.296 g, 1.00 mmol) and the solution heated to reflux for 3 hours during which time it turned pale yellow. The solution was then cooled to room temperature and the thionyl chloride removed by vacuum distillation to give a sticky white solid. This was dissolved in THF (30 mL) and added dropwise to a solution of ethylamine (2 mL, 68 – 72% in water) in THF (5 mL) in an ice-bath. After stirring at this temperature for 5 minutes, the solution was allowed to warm to room temperature over 2 hours during which time a white suspension formed. This was taken to dryness under reduced pressure to give a yellow. This was dissolved in $HCl_{(aq)}$ (1 M, 5 mL) and methanol (10 mL) and then precipitated with THF (200 mL) to give a cloudy suspension, which was stirred at room temperature for 2 hours. The resulting white powder was isolated by filtration, and washed with THF (3 × 10 mL) to give **^{Et}biphen·Cl_2** contaminated with ethylammonium chloride. This was dissolved in water (10 mL) and added to a solution of NaOH (1 M, 10 mL) resulting in the formation of a white powder, which was isolated by filtration and washed with water (5 × 5 mL). It was then dissolved in $HCl_{(aq)}$ (1 M, 5 mL) and methanol (10 mL) and added to THF (200 mL) resulting in a cloudy suspension. This was stirred at room temperature for 2 hours resulting in the formation of a white powder that was isolated by filtration, washed with THF (3 × 10 mL) and dried thoroughly *in vacuo* to give **^{Et}biphen·Cl_2**. Yield: 0.328 g (0.776 mmol, 78%).

^{1}H NMR (d_6-DMSO): 9.68 (tr, *J* = 5.6 Hz, 2H), 9.45 (tr, *J* = 5.7 Hz, 2H), 8.01 (d, *J* = 8.5 Hz, 4H), 7.74 (d, *J* = 8.5 Hz, 4H), 3.45 (dq, *J* = 7.2, ~ 6 Hz, 4H), 3.20 (dq, *J* = 7.2, ~ 6 Hz, 4H), 1.25 (t, *J* = 7.2 Hz, 6H), 1.12 (t, *J* = 7.2 Hz, 6H) ppm. ^{13}C{^{1}H} NMR: 162.6, 141.9, 129.0, 128.3, 127.5, 37.8, 15.2, 12.9 ppm (one peak not observed, likely due to overlap with NMR solvent peak). HRESI-MS (pos.): *m/z* = 176.1316, calc. for $[C_{22}H_{32}N_4]^{2+}$ = 176.1308. ATR-IR (*inter alia*): 1644 (strong) cm^{-1}.

Synthesis of ^{Et}tetra-amide: Thionyl chloride (3 mL) was added to tetrakis(carboxyphenyl)methane (0.248 g, 0.500 mmol), and DMF (3 drops) was added cautiously. The mixture was heated to reflux under N_2 overnight, during which time all material dissolved to give a clear colourless solution. The reaction was then cooled to room temperature and thionyl chloride was removed by vacuum distillation to give a waxy white solid. This was dissolved in THF (15 mL) and added over approximately 2 minutes to ethylamine solution (2 mL, 68 – 72% in water) in THF (5 mL) in an ice-bath. Stirring was continued in the ice-bath for 5 minutes and then the white suspension allowed to warm to room temperature over an hour. Water was added (20 mL) causing the formation of a clear colourless solution, to which was added $HCl_{(aq)}$ (1 M, 20 mL) resulting in the formation of a white precipitate. The THF was removed on a rotary evaporator and then the white aqueous suspension was filtered to give a white powder, which was washed with water (5 × 10 mL) and dried thoroughly *in vacuo* to give **^{Et}tetra-amide**. Yield: 0.273 g (0.452 mmol, 90%).

^{1}H NMR (d_6-DMSO): 8.43 (t, *J* = 5.6 Hz, 4H), 7.75 (d, *J* = 8.3 Hz, 8H), 7.28 (d, *J* = 8.3 Hz, 8H), 3.26 (dq, *J* = 7.1, 5.6 Hz, 8H), 1.09 (t, *J* = 7.1 Hz, 12H) ppm. ^{13}C{^{1}H} NMR (d_6-DMSO): 165.6, 148.4, 132.7, 130.1, 127.0, 64.6, 34.0, 14.8 ppm. HRESI-MS (pos.): *m/z* = 627.2936, calc. for $[C_{37}H_{40}N_4O_4{\cdot}Na]^+$ = 627.2942. ATR-IR (*inter alia*): 1620 (strong), 1545 (strong) cm^{-1}.

Synthesis of ^{Et}tetra·Cl_4: Thionyl chloride (3 mL) was added to **^{Et}tetra-amide** (0.151 g, 0.250 mmol) and the mixture heated to reflux for 5 hours, during which time all material dissolve to give a clear, pale yellow solution. Upon cooling this formed a white suspension; the thionyl chloride was removed by vacuum distillation to give a waxy white solid. This was suspended in THF (45 mL), and sonicated to give a fine white suspension. The suspension was added to a solution of ethyl amine (2 mL, 68 – 72% in water) in THF (5 mL) in an ice-bath. The resulting slightly cloudy white suspension was allowed to warm to room temperature overnight during which time all material dissolved to give a clear colourless solution with a small amount of an insoluble oil. The THF was removed on a rotary evaporator to give a yellow liquid. $NaOH_{(aq)}$ (1 M, 20 mL) was added to this to give a white suspension, which was filtered to give a white powder that was washed with water (3 × 5 mL). This powder was dissolved using $HCl_{(aq)}$ (1 M, 12 mL) and then this was blown down under N_2 to give a glassy solid. This was taken up in EtOH (10 mL) and added to Et_2O (30 mL), which initially gave a milky suspension that soon settled to give a yellow oil and colourless supernatant. The supernatant was decanted and EtOH:Et_2O (1:3, 20 mL) was added and the mixture stirred for 3 hours. Again the supernatant was decanted to give a gunky solid. EtOAc (5 mL) was added to this, and the white suspension sonicated for 30 minutes. The EtOAc was then blown off under N_2 to give a white powder, which was thoroughly dried *in vacuo* to give **^{Et}tetra·Cl_4**. Yield: 0.124 g (0.144 mmol, 58%).

^{1}H NMR (d_6-DMSO): 9.74 – 9.79 (m, 8H), 7.63 (d, *J* = 8.1 Hz, 8H), 7.39 (d, *J* = 8.1 Hz, 8H), 3.49 (dq, *J* = 7.1, ~ 6 Hz, 8H), 3.19 (dq, *J* = 7.1, ~ 6 Hz, 8H) 1.21 (t, *J* = 7.1 Hz, 12H), 1.12 (t, *J* = 7.1 Hz, 12H) ppm. ^{13}C{^{1}H} NMR (d_6-DMSO): 162.2, 148.3, 130.7, 128.2, 126.9, 64.7, 37.9, 15.2, 13.0 ppm (one peak not observed, likely due to overlap with NMR solvent peak). HRESI-MS (pos.): *m/z* = 357.2563, calc. for $[C_{45}H_{62}N_8]^{2+}$, *i.e.* loss of 2 H^+ and 4 Cl^- = 357.2542; 238.5067, calc. for $[C_{45}H_{63}N_8]^{3+}$, *i.e.* loss of H^+ and 4 Cl^- = 238.5053. ATR-IR (*inter alia*): 1634 (strong) cm^{-1}.

Synthesis of ^{Et}biphen·TP: A solution of **TBA_2·TP** (52 mg, 80 µmol) in ethanol (2 mL) was added to a solution of **^{Et}biphen·Cl_2** (34 mg, 80 µmol) in ethanol (2 mL) and the resulting colourless solution left to stand at room temperature. Within 3 – 4 days crystals were visible, and after 14 days the crystals were isolated by filtration, washed with ethanol (2 × 1 mL) and thoroughly air-dried to give **^{Et}biphen·TP**. Yield: 15 mg (29 µmol, 36%).

^{1}H NMR (d_6-DMSO containing a drop of $DCl_{(aq)}$): 9.69 – 9.74 (m, 4H), 8.02 (s, 4H), 7.98 (d, *J* = 8.4 Hz, 4H), 7.72 (d, *J* = 8.4 Hz, 4H), 3.46 – 3.53 (m, 4H), 3.15 – 3.21 (m, 4H), 1.23 (t, *J* = 7.2 Hz, 6H), 1.10 (t, *J* = 7.2 Hz, 6H) ppm. ATR-IR (*inter alia*): 1664 (strong), 1371 (strong), 1343 (strong) cm^{-1}. A PXRD trace is provided in the ESI (Figure S20).

Synthesis of ^{Et}tetra·TC: A solution of **TBA_4·TC** (37 mg, 25 µmol) in ethanol (2.5 mL) was added to a solution to **^{Et}tetra·Cl_4** (21 mg, 25 µmol) in ethanol (2.5 mL) causing a slight cloudiness to appear. Over the course of a few days standing at room temperature, the solution cleared and crystals appeared. After ten days, these were isolated by filtration, washed with ethanol (4 × 1 mL) and thoroughly air-dried to give **^{Et}tetra·TC**. Yield: 28 mg (23 µmol, 92%).

^{1}H NMR (d_6-DMSO containing a drop of $DCl_{(aq)}$): 9.70 – 9.77 (m, 8H*), 7.88 (d, *J* = 8.6 Hz, 8H), 7.61 (d, *J* = 8.2 Hz, 8H), 7.37 (d, *J* = 8.2 Hz, 8H), 7.32 (d, *J* = 8.6 Hz, 8H), 3.44 – 3.50 (m, 8H), 3.13 – 3.20 (m, 8H), 1.19 (t, *J* = 7.2 Hz, 12H), 1.09 (t, *J* = 7.2 Hz, 12H) ppm. ATR-IR (*inter alia*): 1638 (strong), 1587 (strong), 1538 (strong), 1368 (strong) cm^{-1}. A PXRD trace is provided in the ESI (Figure S23). * Actual integration is lower than this, which we attribute to H/D exchange.

Synthesis of ^{Et}biphen·BPDC and **^{Et}tetra·(^{H}BPDC)$_4$:** Despite numerous attempts we were only ever able to isolate small quantities of these compounds. In the case of **^{Et}biphen·BPDC**, we could reproducibly obtain a small number of crystals but never in high enough yield to make characterisation of bulk product possible. In the case of **^{Et}tetra·(^{H}BPDC)$_4$**, we initially obtained a modest yield of crystals, but attempts to reproduce the synthesis gave only amorphous material. See Tables S2 and S5 for more information.

Conflicts of interest

There are no conflicts to declare.

Data availability

Crystallographic data in CIF format have been deposited with the Cambridge Crystallographic Data Centre (CCDC: 2503994 – 2503998). Other data are provided in the ESI.

Acknowledgements

We thank the Australian Research Council for funding this work (FT210100495 to NGW). This research was undertaken in part using the MX2 beamline[53] at the Australian Synchrotron, part of ANSTO, and made use of the Australian Cancer Research Foundation detector.

Notes and references

1 M. Simard, D. Su and J. D. Wuest, *J. Am. Chem. Soc.*, 1991, **113**, 4696–4698.
2 O. Ermer and L. Lindenberg, *Helv. Chim. Acta*, 1991, **74**, 825–877.
3 R.-B. Lin, Y. He, P. Li, H. Wang, W. Zhou and B. Chen, *Chem. Soc. Rev.*, 2019, **48**, 1362–1389.
4 N. G. White and C. M. McGuirk, *Chem. Soc. Rev.*, 2025, **54**, 9612–9629.
5 These frameworks have sometimes been referred to by other names including iHOF (ionic Hydrogen-bonded Organic Framework), CPOS (Crystalline Porous Organic Salt) or non-MOF (non-Metal Organic Framework). In a recent review, White and McGuirk argued that having multiple names for the same class of framework is unhelpful and suggested consolidating nomenclature around the term HOF (see Ref. 4).
6 V. A. Russell, C. C. Evans, W. Li and M. D. Ward, *Science*, 1997, **276**, 575–579.
7 T. Adachi and M. D. Ward, *Acc. Chem. Res.*, 2016, **49**, 2669–2679.
8 M. O'Shaughnessy, J. Glover, R. Hafizi, M. Barhi, R. Clowes, S. Y. Chong, S. P. Argent, G. M. Day and A. I. Cooper, *Nature*, 2024, **630**, 102–108.
9 M. O'Shaughnessy, H. Qu, X. Wang, J. B. Holmes, L. Emsley, J. Glover, R. Hafizi, G. M. Day and A. I. Cooper, *J. Am. Chem. Soc.*, 2025, **147**, 39351–39358.
10 H. Wahl, D. A. Haynes and T. le Roex, *Chem. Commun.*, 2012, **48**, 1775–1777.
11 N. Roques, G. Mouchaham, C. Duhayon, S. Brandès, A. Tachon, G. Weber, J. P. Bellat and J.-P. Sutter, *Chem. Eur. J.*, 2014, **20**, 11690–11694.
12 G. Xing, I. Bassanetti, T. Ben, S. Bracco, P. Sozzani, L. Marchiò and A. Comotti, *Cryst. Growth Des.*, 2018, **18**, 2082–2092.
13 G. Xing, I. Bassanetti, S. Bracco, M. Negroni, C. Bezuidenhout, T. Ben, P. Sozzani and A. Comotti, *Chem. Sci.*, 2019, **10**, 730–736.
14 G. Xing, T. Yan, S. Das, T. Ben and S. Qiu, *Angew. Chem. Int. Ed.*, 2018, **57**, 5345–5349.
15 T. Miyano, N. Okada, R. Nishida, A. Yamamoto, I. Hisaki and N. Tohnai, *Chem. – Eur. J.*, 2016, **22**, 15430–15436.
16 T. Ami, K. Oka, K. Tsuchiya and N. Tohnai, *Angew. Chem. Int. Ed.*, 2022, **61**, e202202597.
17 M. W. Hosseini, R. Ruppert, P. Schaeffer, A. De Cian, N. Kyritsakas and J. Fischer, *J. Chem. Soc. Chem. Commun.*, 1994, 2135–6.
18 O. Félix, M. W. Hosseini, A. De Cian and J. Fischer, *Angew. Chem. Int. Ed. Engl.*, 1997, **36**, 102–104.
19 S. Lie, T. Maris, C. Malveau, D. Beaudoin, F. Helzy and J. D. Wuest, *Cryst. Growth Des.*, 2013, **13**, 1872–1877.
20 M. Morshedi, M. Thomas, A. Tarzia, C. J. Doonan and N. G. White, *Chem. Sci.*, 2017, **8**, 3019–3025.
21 D. A. Cullen, M. G. Gardiner and N. G. White, *Chem. Commun.*, 2019, **55**, 12020–12023.
22 N. A. Tzioumis, D. A. Cullen, K. A. Jolliffe and N. G. White, *Angew. Chem. Int. Ed.*, 2023, **62**, e202218360.
23 S. A. Boer, M. Morshedi, A. Tarzia, C. J. Doonan and N. G. White, *Chem. Eur. J.*, 2019, **25**, 10006–10012.
24 N. G. White, *Chem. Commun.*, 2021, **57**, 10998–11008.
25 M. Wang, J. Tang, J. Liu, Q. Zheng, W. Li, J. Sheng and L. Mao, *Angew. Chem. Int. Ed.*, 2021, **60**, 22315–22321.
26 S. Lie, T. Maris and J. D. Wuest, *Cryst. Growth Des.*, 2014, **14**, 3658–3666.
27 A. R. Y. Almuhana, G. R. F. Orton, C. Rosenberg and N. R. Champness, *Chem. Commun.*, 2024, **60**, 452–455.
28 A. R. Y. Almuhana, S. L. Griffin and N. R. Champness, *CrystEngComm*, 2024, **26**, 4643–4648.
29 P. Muang-Non and N. G. White, *Cryst. Growth Des.*, 2024, **24**, 8135–8144.
30 S. Zhang, J. Fu, S. Das, K. Ye, W. Zhu and T. Ben, *Angew. Chem. Int. Ed.*, 2022, **61**, e202208660.
31 P. Muang-Non, C. Richardson and N. G. White, *Angew. Chem. Int. Ed.*, 2023, **62**, e202212962.
32 P. Muang-Non, A. W. Markwell-Heys, C. J. Doonan and N. G. White, *Chem. Commun.*, 2023, **59**, 4059–4062.
33 R. J. Goodwin, P. Muang-Non, N. A. Tzioumis, K. A. Jolliffe and N. G. White, *Chem. – Eur. J.*, 2025, **31**, e202404208.
34 W. Liang, F. Carraro, M. B. Solomon, S. G. Bell, H. Amenitsch, C. J. Sumby, N. G. White, P. Falcaro and C. J. Doonan, *J. Am. Chem. Soc.*, 2019, **141**, 14298–14305.
35 F. Carraro, M. Aghito, S. Dal Zilio, H. Wolinski, C. J. Doonan, B. Nidetzky and P. Falcaro, *Small*, 2024, **20**, 2407487.
36 Y. Tanaka, H. Katagiri, Y. Furusho and E. Yashima, *Angew. Chem. Int. Ed.*, 2005, **44**, 3867–3870.
37 H. Katagiri, Y. Tanaka, Y. Furusho and E. Yashima, *Angew. Chem. Int. Ed.*, 2007, **46**, 2435–2439.
38 A. Kraft, L. Peters and H. R. Powell, *Tetrahedron*, 2002, **58**, 3499–3505.
39 M. P. Coles, F. A. Stokes, B. F. K. Kingsbury, B. M. Day and P. B. Hitchcock, *Cryst. Growth Des.*, 2011, **11**, 3206–3212.
40 T. Kusukawa, K. Inoue, H. Obata and R. Mura, *Tetrahedron*, 2017, **73**, 661–670.
41 M. K. S. Perry-Britton and N. G. White, *Cryst. Growth Des.*, 2025, **25**, 9876–9885.
42 L. Pop, N. D. Hadade, A. van der Lee, M. Barboiu, I. Grosu and Y.-M. Legrand, *Cryst. Growth Des.*, 2016, **16**, 3271–3278.
43 *Bindfit*, accessed at supramolecular.org.
44 S. Alvarez, *Dalton Trans.*, 2013, **42**, 8617–8636.
45 A. L. Spek, *Acta Crystallogr.*, 2015, **C71**, 9–18.
46 W. Zhao, A. H. Flood and N. G. White, *Chem. Soc. Rev.*, 2020, **49**, 7893–7906.
47 N. G. White, *CrystEngComm*, 2019, **21**, 4855–4858.
48 R. Taylor and P. A. Wood, *Chem. Rev.*, 2019, **119**, 9427–9477.
49 Y. Zhao and D. G. Truhlar, *Theor. Chem. Acc.*, 2008, **120**, 215–241.
50 J.-D. Chai and M. Head-Gordon, *Phys. Chem. Chem. Phys.*, 2008, **10**, 6615.
51 A. J. Lowe and F. M. Pfeffer, *Chem. Commun.*, 2008, 1871–1873.
52 S. A. Boer, L. Conte, A. Tarzia, M. T. Huxley, M. G. Gardiner, D. R. T. Appadoo, C. Ennis, C. J. Doonan, C. Richardson and N. G. White, *Chem. Eur. J.*, 2022, **28**, e202201929.
53 D. Aragao, J. Aishima, H. Cherukuvada, R. Clarken, M. Clift, N. P. Cowieson, D. J. Ericsson, C. L. Gee, S. Macedo, N. Mudie, S. Panjikar, J. R. Price, A. Riboldi-Tunnicliffe, R. Rostan, R. Williamson and T. T. Caradoc-Davies, *J. Synchrotron Radiat.*, 2018, **25**, 885–891.